JTTEE5 6:425-429
©ASM International

A Transmission Electron Microscopy Study of the Microstructures Present in Alumina Coatings Produced by Plasma Spraying

J.M. Guilemany, J. Nutting, and M.J. Dougan

(Submitted 17 June 1996; in revised form 14 June 1997)

Alumina coatings deposited onto steel substrates by plasma spraying were studied using transmission electron microscopy. A number of allotropes of alumina distinct from the alpha-alumina of the starting powder were identified. The as-sprayed coatings consist primarily of metastable gamma-alumina and amorphous/nanocrystalline material. Areas of alpha-alumina were observed, generally in conjunction with the twinned metastable phases delta- and theta-alumina, and these were interpreted as resulting from solid-state transformation from the gamma phase, due to the annealing action of subsequent passes of the plasma torch. The absence of such phases from the first- and last-deposited layers is further evidence for such a mechanism.

Keywords alumina coatings, metastable phases, microscopy, structure

1. Introduction

Plasma-sprayed alumina coatings are used in a variety of applications, to provide electrical insulation, increased wear resistance, or a chemically unreactive surface. The macrostructure of such coatings is fairly well established as consisting of lamellae built up from the molten droplets impinging on the substrate (Ref 1). It has further been found that a number of different allotropes of alumina can be produced in such coatings (Ref 2). However, there appears to have been relatively little investigation into the microstructures within the solidified splats. The object of the present work was to investigate the types and distributions of microstructures present in plasma-sprayed alumina coatings, using transmission electron microscopy (TEM).

2. Experimental Procedure

Samples were prepared by plasma spraying alumina powder onto a low-alloy steel substrate, ($34CrMo_4$ UNS-G41350, containing 0.37 wt% C and 0.97 wt% Cr) using Plasma Technik (Sulzer Metco) A3000 equipment with an F4 gun. The feedstock was Amdry 99.5% alpha-alumina with a particle size of +45 to 22 μm. In order to improve the coating-substrate adhesion, the substrate surface was roughened prior to spraying by grit blasting with corundum, so that the surface roughness (R_a) was about 4 μm. The total thickness of the sprayed coating was about 300 μm.

J.M. Guilemany, J. Nutting, and **M.J. Dougan,** Centre de Proyeccion Térmica, Dept. de Ingeniería Química y Metalurgia, Facultat de Química, Universitat de Barcelona, Martí i Franqués 1, 08028-Barcelona, Spain.

X-ray powder diffraction (XRD) analysis, with both Co and Cu Kα radiation, was used to determine the types and proportions of phases present in the as-sprayed coating. Scanning electron microscopy (SEM) and TEM were used to observe the coating structure.

Thin-foil samples were prepared to allow TEM examination of the coating and coating-substrate interface using methods described elsewhere (Ref 3). TEM examination was carried out using a Hitachi H800MT TEM-STEM at an accelerating voltage of 200 kV.

3. Results and Discussion

XRD analysis of several similar coatings suggested that each consisted of gamma- and alpha-alumina. Gamma-alumina is a metastable phase, frequently found in flame-sprayed alumina coatings, which experience rapid rates of cooling from the molten state.

A typical XRD trace is shown in Fig. 1. The proportions of the phases were calculated from the ratios of the heights of the {113} alpha and {440} gamma peaks. The results obtained ranged between 17 and 23% alpha-alumina, with the remainder gamma phase.

SEM examination of the coatings showed the expected lamellar arrangement (Fig. 2). The most frequently observed structures in TEM examination of the coatings were columnar grains (Fig. 3). These varied in size and appeared to be aligned perpendicular to the interface with the previous layer, and therefore parallel to the direction of heat removal. Where impingement of a splat had occurred with a curved or irregular surface, this led to radial arrangements of columns (Fig. 4). Analysis of selected-area diffraction (SAD) patterns from these areas (Fig. 5) showed them to be gamma-alumina, with a face-centered cubic structure (Ref 4).

In conjunction with these columnar areas, amorphous or nanocrystalline regions were also frequently observed, giving diffuse rings in the SAD pattern. This was the predominant

structure observed at the coating-substrate interface (Fig. 6), and it was seen throughout the coating at the interfaces between subsequent layers. Clearly these locations correspond to the deposition of molten material on relatively cold surfaces, and therefore to the most rapid rates of cooling, which will lead to the suppression of nucleation. It was also found that amorphous alumina and columnar gamma-alumina could coexist within the same splat (Fig. 7). This presumably results from the lowering of the cooling rate for the part of a splat furthest from the substrate, due to the amorphous material acting as a barrier to heat flow, to a rate insufficient to form an amorphous structure. A band of fine crystalline material is formed adjacent to the amorphous layer, and then, as the cooling rate becomes even lower, columnar crystals of alumina are formed adjacent to the fine crystalline layer.

No evidence was seen for any intermediate phase between the steel substrate and the amorphous alumina at the interface, and this is consistent with the poor adhesive strength of such metal-ceramic systems (typically around 12 MPa), which results from purely mechanical bonding between the coating and the pre-roughened substrate.

Also occasionally observed in these amorphous areas were nanocrystallites, of up to approximately 60 nm in size, which gave rise to spotty rings in the SAD diffraction pattern corre-

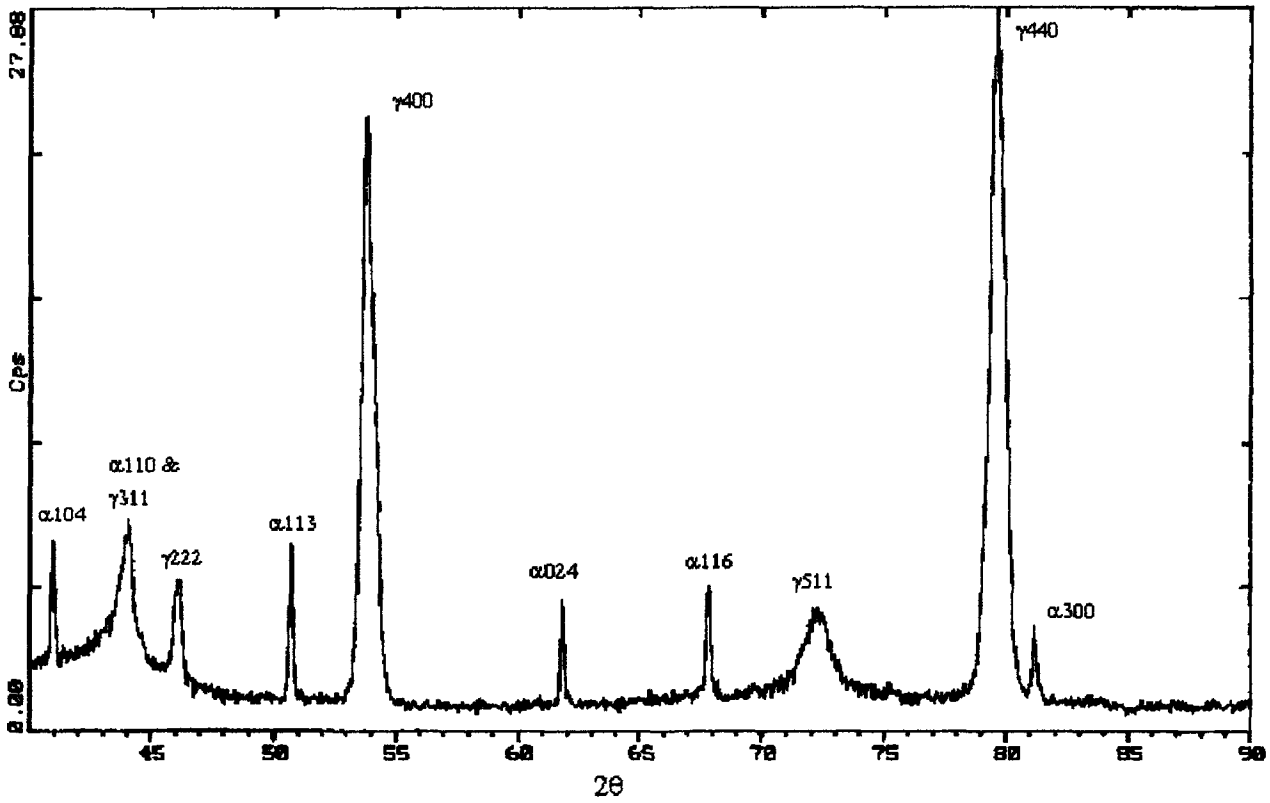

Fig. 1 XRD diffraction spectrum from as-sprayed alumina coating (Cu Kα radiation)

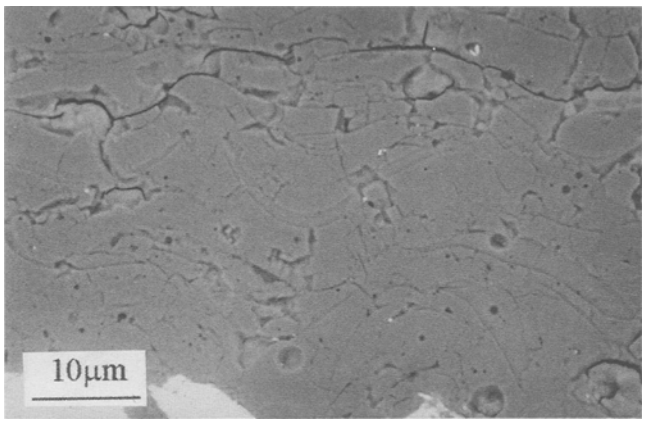

Fig. 2 SEM micrograph showing lamellar structure of alumina coating

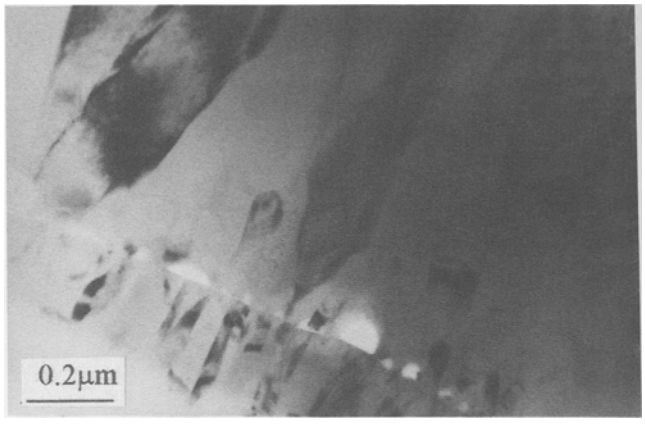

Fig. 3 TEM micrograph showing columnar grain structure of γ-Al_2O_3

sponding to the {400} and {440} gamma-alumina reflections (Fig. 8a, b). It is difficult to be certain of the extent to which these occur as a result of the spraying process. The observation was made that the nucleation of such nanocrystallites in amorphous material could occur in situ, under the action of the electron beam in the TEM.

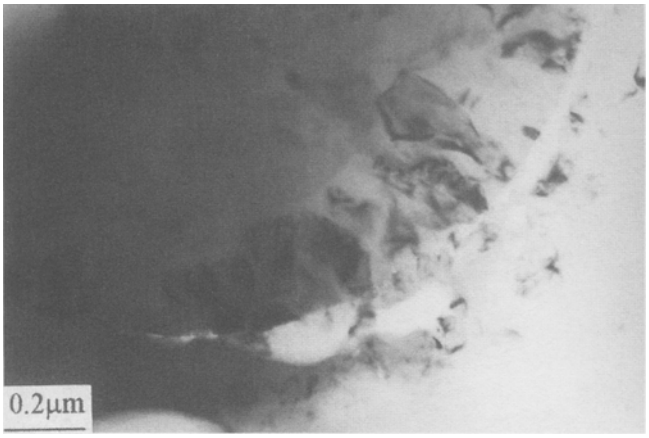

Fig. 4 TEM micrograph showing columns arranged radially, perpendicular to the interface with the previously deposited splat

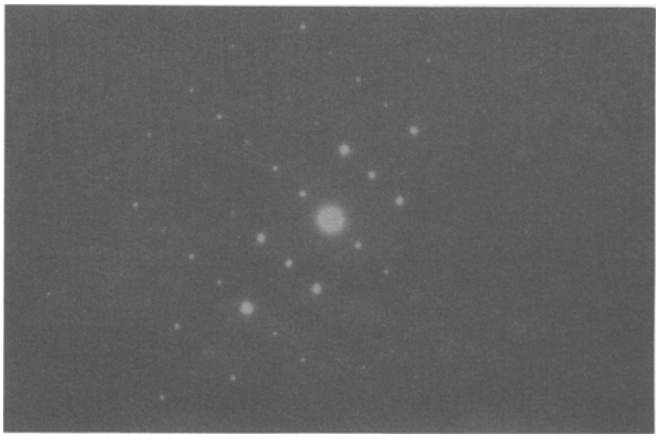

Fig. 5 Selected area diffraction pattern from gamma-alumina

Fig. 6 TEM micrograph showing amorphous alumina (A) and steel substrate (S). The steel has a martensitic structure

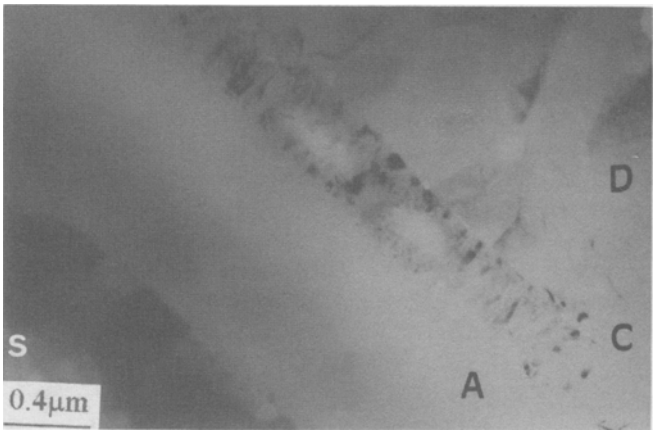

Fig. 7 TEM micrograph showing interface between steel substrate (S) and amorphous alumina region (A). The diagonal band running across the micrograph is a crystalline region (C). Adjacent to this band there are columnar crystals of alumina (D)

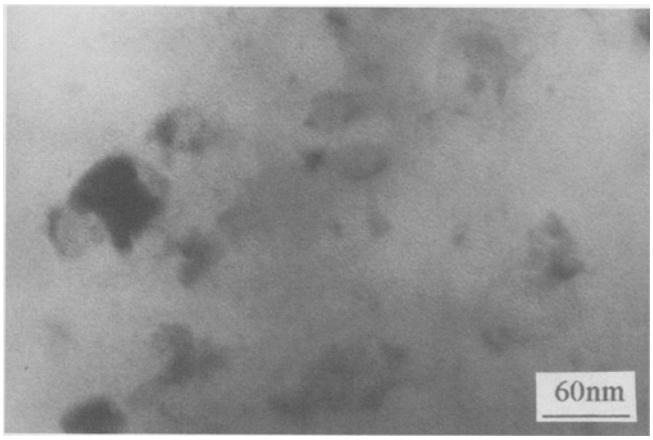

(a)

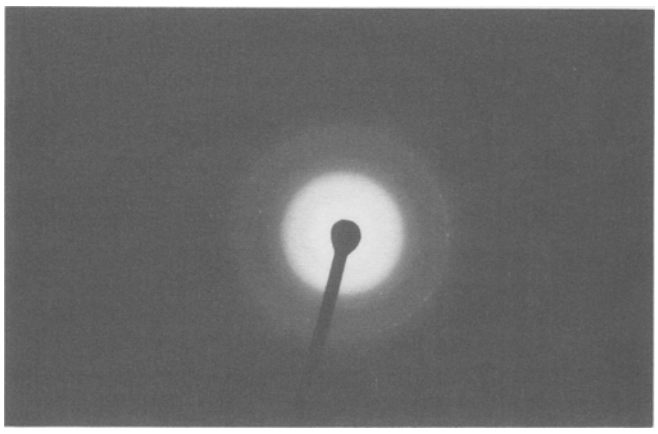

(b)

Fig. 8 (a) TEM micrograph showing an amorphous area of alumina containing nanocrystallites of γ-Al_2O_3. (b) Selected area diffraction pattern from a region in (a). Note γ-alumina spotty rings corresponding to the {400} and {440} planes.

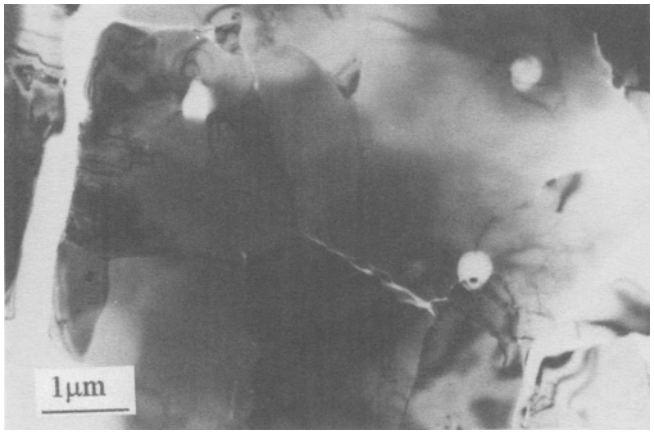

Fig. 9 TEM micrograph showing a region of equiaxed α-Al_2O_3 grains

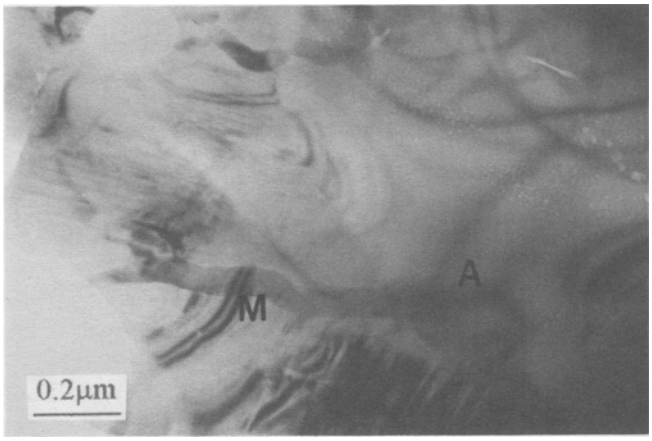

Fig. 10 TEM micrograph showing twinned metastable regions (M) adjacent to a grain of α-Al_2O_3 (A)

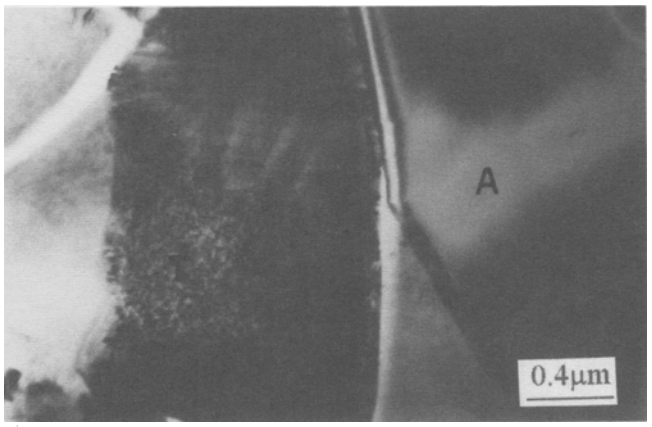

(a)

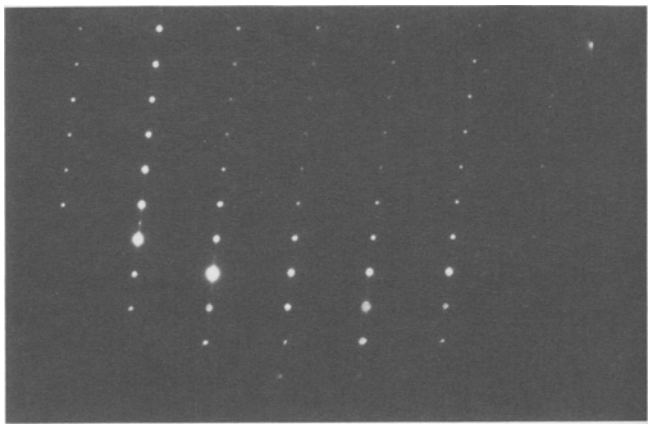

(b)

Fig. 11 (a) TEM micrograph showing twinned θ-Al_2O_3 (T) adjacent to α-Al_2O_3 (A). (b) Selected area diffraction pattern from θ-Al_2O_3

Areas of equiaxed grains were also observed in the coatings (Fig. 9), and these were shown by analysis of SAD patterns to be alpha-alumina (Ref 5). It has been suggested that the alpha-alumina content of plasma-sprayed alumina coatings results from the incorporation of unmolten starting powder. While this undoubtedly accounts for some of the alpha-alumina found by XRD, the evidence suggests that the alpha-alumina observed in the TEM in the present work is the result of solid-state transformation from gamma-alumina subsequent to the initial deposition.

The equiaxed areas generally show some cracking at the grain boundaries (Fig. 9). Gamma-alumina is a defect spinel of the form $AlO{\cdot}Al_2O_3$, with a lower density than alpha-alumina, and the gamma-alpha transformation is accompanied by a volume contraction that can cause grain boundary cracking. Such transformed areas are undesirable because they adversely affect the mechanical properties of the coating. Thin foils from alumina are difficult to prepare and cracks may form as a result of ion milling. These cracks are usually along the edge of the foil. The cracks shown in Fig. 9 are not along the edge of the foil, but they are present in regions where the stress is likely to be high from the volume changes.

The most compelling reason for believing the alpha-alumina observed here to be the result of transformation from gamma phase is the observation of some heavily twinned areas between the columnar gamma and equiaxed alpha regions (Fig. 10). Some of these resemble regions observed by Bhatkal et al. (Ref 6) in similar coatings. In the present work these areas have been found by SAD pattern analysis to consist of both tetragonal delta-alumina (Fig. 11a, b) and monoclinic theta-alumina (Fig. 12) (Ref 7, 8). Both of these phases are metastable defect spinels intermediate between gamma- and alpha-alumina, and the gamma-alpha transformation occurs by the progressive ordering of defects.

It has been proposed that transformation from gamma- to alpha-alumina in such coatings is most likely to occur at the coating-substrate interface, where, it is suggested, the coating will experience the greatest annealing due to heating by the subsequent layers (Ref 9). However, in the present work equiaxed areas were observed only in the main body of the coating, that is to say, not in the first or last layers deposited. This is presumably due to the relatively poor thermal conductivity of alumina. The middle layers of the coating experience lower rates of heat removal than those adjacent to the substrate, which will act as a

heat sink, while the last-deposited layer will not receive any subsequent annealing.

Ramm et al. (Ref 10) measured the alpha-alumina content of coatings produced by both plasma and high-velocity oxygen fuel (HVOF) spraying, using a variety of techniques. They consistently found the HVOF-sprayed coatings to contain a lower proportion of alpha-alumina than those produced by plasma spraying, and they suggested that this might be due to more complete melting of the starting powder in the HVOF process. However, in light of the results found here, it seems more probable that the lower temperature of the HVOF process led to less self-annealing of the coating, and consequently to less transformation from gamma- to alpha-alumina.

No TEM evidence was found to support the idea that unmelted alpha-alumina from the starting powder is incorporated into the coating. However, it is recognized that the large size of unmelted particles makes them particularly prone to drop-out during sample preparation.

4. Conclusions

- The plasma-sprayed alumina coatings examined here contain three principal structures.
- Deposition of the molten material directly on the substrate, or on relatively cold previously deposited alumina, leads to the formation of an amorphous phase.
- The majority of the coating nucleates as gamma-alumina to give a structure of columnar grains.
- The annealing action of subsequently deposited layers leads to solid-state transformation in the main body of the coating and to the formation of areas of equiaxed alpha-alumina.

Acknowledgments

MJD thanks the European Union for the Human Capital Mobility award No. ERBCHBGCT920044. JN acknowledges the Sabbatical Year Concession SAB-930020. The authors also thank the Generalitat de Catalunya, for funding under Project 1995SGR00423, and Dr. J.R. Miguel and Dr. M.D. Nuñez for their help in spraying the samples.

References

1. R. McPherson, A Review of Microstructure and Properties of Plasma-Sprayed Ceramic Coatings, *Surf. Coat. Technol.*, Vol 39/40, 1989, p 173-181

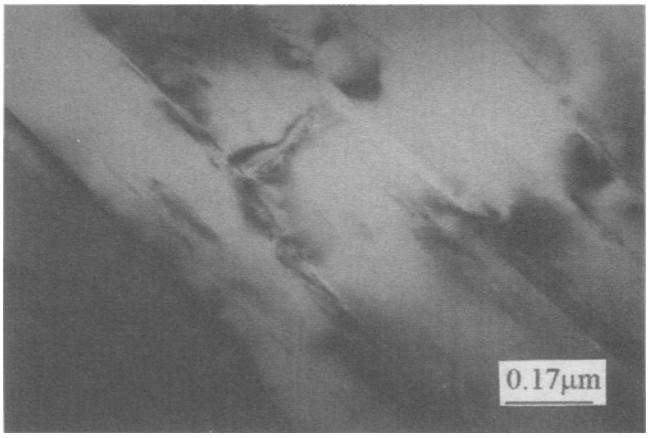

Fig. 12 TEM micrograph showing twinned δ-Al_2O_3

2. G.N. Heintze and S. Uematsu, Preparation and Structures of Plasma-Sprayed γ- and α-Al_2O_3 Coatings, *Surf. Coat. Technol.*, Vol 50, 1992, p 213-222
3. H. Zhang, Preparation of Cross-Sections of Thermal Spray Coatings for TEM Investigations, *J. Thermal Spray Technol.*, Vol 1 (No. 1), March 1992, p 83-88
4. Joint Committee on Powder Diffraction Standards, Powder Diffraction File, Card 10-425, International Centre for Diffraction Data, Swarthmore, PA, 1990
5. Joint Committee on Powder Diffraction Standards, Powder Diffraction File, Card 42-1468, International Centre for Diffraction Data, Swarthmore, PA, 1990
6. R.M. Bhatkal and K. Rajan, Enhancement of Heat-Exchanger Surfaces: Interfacial Reactions during Thermal Spraying, *Thermal Spray Industrial Applications,* C.C. Berndt and S. Sampath, Ed., ASM International, 1994, p 141-146
7. Joint Committee on Powder Diffraction Standards, Powder Diffraction File, Card 16-394, International Centre for Diffraction Data, Swarthmore, PA, 1990
8. Joint Committee on Powder Diffraction Standards, Powder Diffraction File, Card 35-121, International Centre for Diffraction Data, Swarthmore, PA, 1990
9. C.W. Anderson and K.H. Heffner, Precision Gas Bearing Plasma-Sprayed Aluminum Oxide Coating Characterization, *Thermal Spray: International Advances in Coatings Technology,* C.C. Berndt, Ed., ASM International, 1992, p 695-704
10. D.A.J. Ramm, T.W. Clyne, A.J. Sturgeon, and S. Dunkerton, Correlations between Spraying Conditions and Microstructure for Alumina Coatings Produced by HVOF and VPS, *Thermal Spray Industrial Applications,* C.C. Berndt and S. Sampath, Ed., ASM International, 1994, p 239-244